AD-A081 391 CALIFORNIA UNIV BERKELEY ELECTRONICS RESEARCH LAB F/G 20/9
ERGODIC ORBITS IN PARTICLE SIMULATIONS OF STRONG ION RINGS,(U)
JUN 79 A FRIEDMAN DE-AS03-76SF00034
UNCLASSIFIED UCB/ERL-M79/41 NL

1 OF 1
AD
A081 391

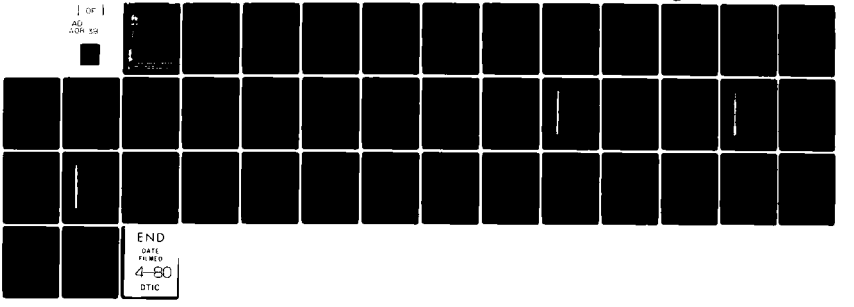

END
DATE FILMED
4-80
DTIC

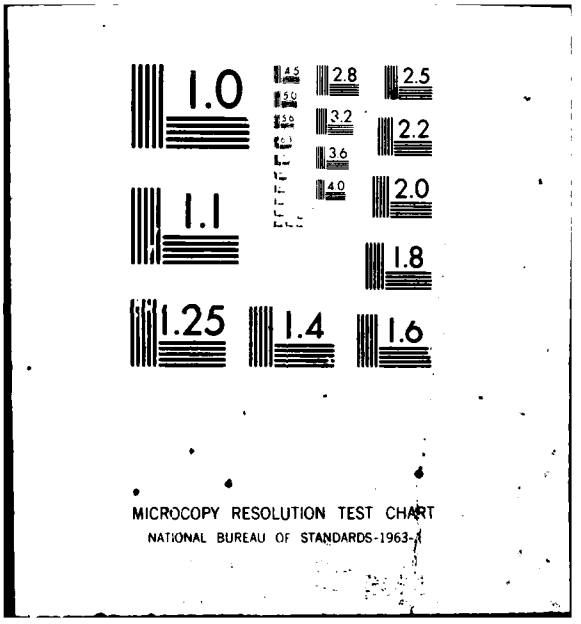
1.0
1.1
1.25
1.4
1.6
1.8
2.0
2.2
2.5
2.8
3.2
3.6
4.0
4.5
5.0
5.6
MICROCOPY RESOLUTION TEST CHART
NATIONAL BUREAU OF STANDARDS-1963-A

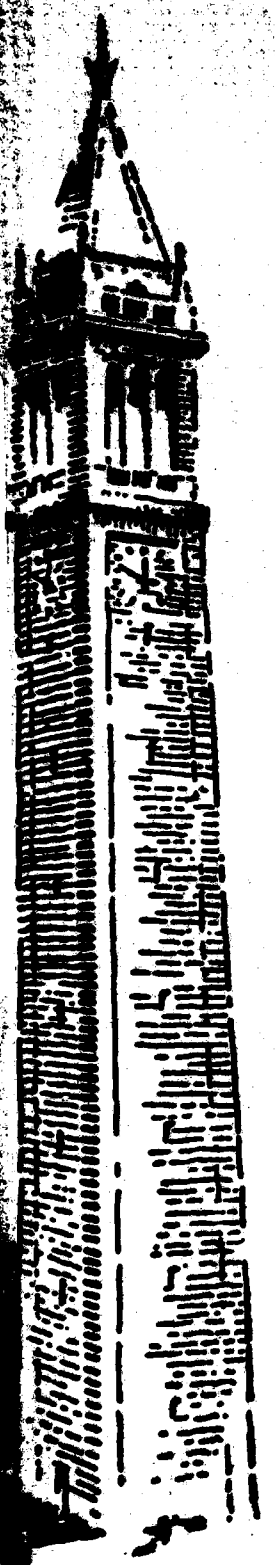







# ERGODIC ORBITS IN PARTICLE SIMULATIONS OF STRONG ION RINGS

by

Alex Friedman

Memorandum No. UCB/ERL M79/41

28 June 1979





ELECTRONICS RESEARCH LABORATORY
College of Engineering
University of California, Berkeley, CA 94720

# ERGODIC ORBITS IN PARTICLE SIMULATIONS OF STRONG ION RINGS •

by

Alex Friedman

28 June 1979

42

Memorandum No. UCB/ERL-M79/41

rept.

28 June 1979

DE-AS03-76SF00034

ELECTRONICS RESEARCH LABORATORY

College of Engineering
University of California, Berkeley
94720

127550

1B

CONTENTS



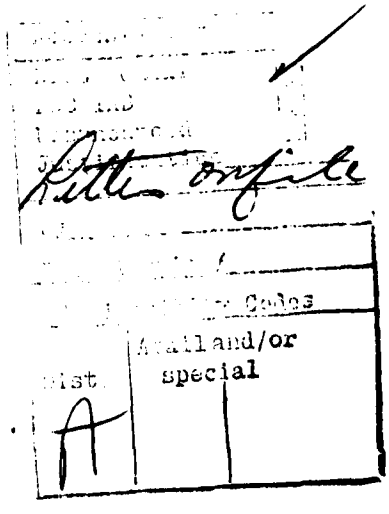

## ABSTRACT

The existence of ergodic orbits in magnetostatic simulations of strong ion rings is demonstrated. For nonlinear 2D3V simulations with axisymmetry the principal manifestation of such orbits is an eventual violation of left-right mirror symmetry in cases where such symmetry would normally be expected, due to the exponential divergence of "neighboring" mirror image trajectories. Linearized simulations, in effect, compute the first order separation of orbits which are displaced from each other by an infinitesimal vector for all time. When a linearized code is applied to a problem involving ergodic orbits, the single-particle growth can be faster than that associated with the collective modes of interest, rendering the simulation invalid. This may severely limit the class of problems for which linearized simulation is applicable. Similar effects are expected in simulations of other systems, including field-reversed mirror equilibria with large nominal gyroradii.

# I. INTRODUCTION

The term "ergodic" is applied to orbits which, loosely speaking, sweep out a nonzero volume of the appropriate phase space. Nonergodic orbits are constrained by an additional constant of the motion to lie on a lower-dimensional surface in this space, and so cannot sweep out a finite volume. Thick ion rings, with aspect ratios of order unity, have been found to include a fraction of ergodic single-particle orbits for moderate values of the field reversal parameter [1]. Some field reversed mirror plasmas may also entail ergodic orbits [1,2]. These configurations are in contrast with infinitesimally-thin "bicycle-tire" rings for which the poloidal angular momentum provides a constant of the motion for all particles, with axially-infinite layers for which the axial angular momentum is conserved, and with those mirror plasmas in which the magnetic moment is an adiabatic invariant. Furthermore, finite-aspect-ratio bicycle-tire rings and noninfinite long layer equilibria, and even certain model thick ion ring equilibria [3], may also contain no ergodic orbits.

One aspect of ergodic-orbit equilibria is of particular concern to simulation models in general and linearized simulations in particular. This is their property of "stochasticity", whereby neighboring trajectories diverge from each other exponentially with time, at least when viewed on a timescale long compared with the system's

characteristic timescale (for ion rings this is the self field betatron timescale). Strictly speaking, stochasticity (in the above sense) is always present when ergodicity is present, but the converse is not true; however, the two terms will be used interchangeably in this discussion.

The RINGHYBRID code [4] is a linearized hybrid code which assumes a nonlinear 2D3V magnetostatic equilibrium. It models the evolution of linearized nonaxisymmetric (3D) perturbations about this equilibrium. Using this code, we have observed, and will present, two manifestations of orbital stochasticity. The first is evident in the zero order motion of particles in an ion ring, appearing as an eventual violation of mirror symmetry about the plane $z = L/2$, and is probably not of serious consequence. We confirm the existence of both ergodic and nonergodic zero order orbits by means of surface of section plots. The second manifestation is a ragged exponential growth of the first-order separation of the displaced and undisplaced particles. Since this growth can be rapid, it can easily mask the behavior of the the collective modes which are the real objects of study in linearized simulation, thereby rendering the simulation invalid.

## II. EFFECTS UPON THE ZERO ORDER SIMULATION

### A. Observation of Ergodicity

The first manifestation of stochasticity is evident in the zero order particle orbits. Particles are injected over a number of timesteps to build up an approximate equilibrium possessing mirror symmetry about the plane $z = L/2$. That is, for each particle with phase-space location $(r_1, z_1, v_{r1}, v_{\theta 1}, v_{z1})$ there is another particle at $(r_2, \ldots) = (r_1, L-z_1, v_{r1}, v_{\theta 1}, -v_{z1})$. Self-consistant fields are calculated using the equation

$$\nabla \times \nabla \times \underline{A} = J_\theta \hat{\theta} - \sigma_0 \dot{\underline{A}},$$

where the last term is used to induce a resistive relaxation toward equilibrium [5]. After allowing the equilibrium to "settle down" and any gross collective oscillations to phase mix out (for perhaps 500 timesteps), fields are "frozen" so that the linearized simulation employs time-invariant "equilibrium" fields. In contrast with the observed behavior of extremely thin bicycle-tire rings wherein left-right mirror symmetry obtains throughout the run, in the thicker rings studied mirror symmetry is seen to persist for a time on the order of 1000 timesteps, after which it is observed to break down for at least some of the particles. This can be interpreted as follows: the mirror image particles are in fact only mirror images to one part in (say) $10^{13}$ - roundoff errors in the computation guarantee that no exact mirror

symmetry can obtain. Thus, except for the axial reflection about L/2, these two orbits can be considered to be "neighboring trajectories". These diverge exponentially in time (with noise superposed), and eventually the difference between the two orbits (i.e., $z_1+z_2-L$) has exponentiated from $10^{-13}$ to unity, and the orbits become visibly different.

A specific example is the run "JVA" (which was re-run as "JWA" with different diagnostics). For this run 2400 simulation particles were employed, the major radius was $r_0=15$, the wall was at $r_w=24$, and the periodicity length L was 24. The radial and axial rms halfwidths were 2.0 and 2.8 respectively (due to finite particle size the effective halfwidths are somewhat larger). The external-field cyclotron period was 40.0, the *mean* gyration period being increased to 42 by self-field effects. A nominal betatron period, obtained by integrating over $J_\theta$ (as in eq. 27 of reference [6]), was 52 timesteps, although axial and radial betatron periods differ greatly for a ring of this geometry. The field reversal factor was 18 percent on axis, and 25 percent immediately under the ring. For this run the convergence criterion for the zero order field-solver was set to EPS=$10^{-13}$, so that the initial symmetry was good to somewhat fewer than 13 digits, taking error propagation on the mesh and the actual magnitude of $A_\theta$ into consideration. The resistive relaxation term $\sigma_0$ was used with a value of .125, and zero order fields were "frozen" at timestep 450.

Snapshots of the ring at timesteps 500 and 2000 are presented in Figs. 1a and 1b respectively. Asymmetries, especially in those particle orbits with large axial excursions, are evident in the plots at IT = 2000.

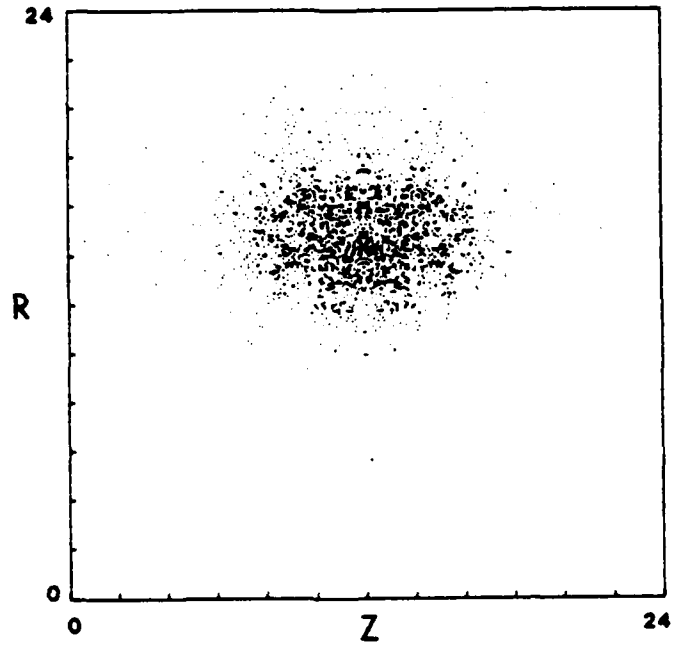


1a. Particle locations in the r – z plane at timestep 500.

Note the absence of assymmetry about z = L/2.

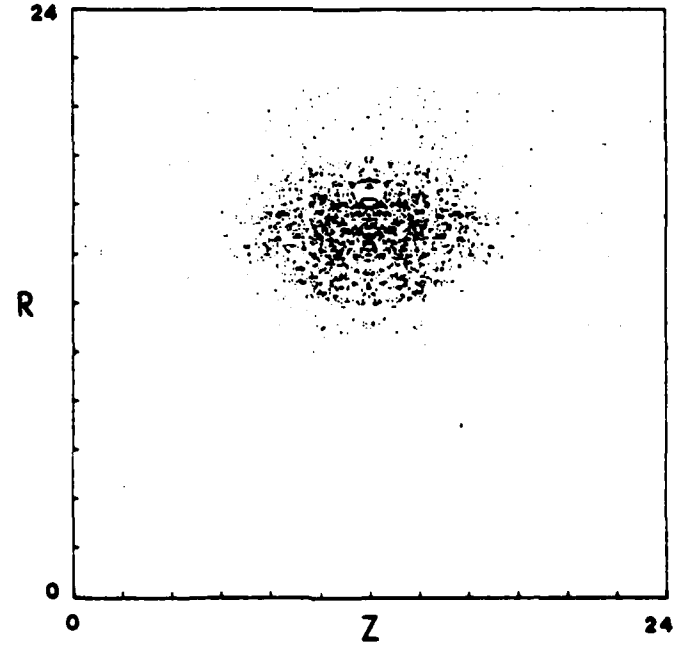


1b. Particle locations in the r – z plane at timestep 2000.

Assymmetry about z = L/2 is now evident.

The second figure shows the orbits of a pair of particles which were initially mirror images of each other. For each particle r and z are plotted as functions of time. Mirror symmetry is seen to obtain until approximately timestep 1100, at which point the orbits become visibly different (much easier to see on a larger plot - on this one the orbits differ visibly only after another 100 timesteps or so). The straight vertical lines are the result of the periodic particle boundary condition being enforced when a particle passes through z = 0 or z = L. Note that this pair of particles was selected to illustrate the eventual breaking of mirror symmetry - not all pairs of particles would have shown this effect.

Using an interactive debugging routine, the quantity $z_1+z_2-L$ was printed out at every other timestep. From this printout the growth rate of the separation of the "neighboring" mirror image orbits could be calculated. The timestep at which each decade of separation was first reached was noted:

| | |
|---|---|
| decade −11 was first reached at | IT = 90 |
| −10 | 230 |
| −9 | 296 |
| −8 | 332 |
| −7 | 404 |
| −6 | 616 |
| −5 | 728 |
| −4 | 764 |
| −3 | 872 |
| −2 | 956 |
| −1 | 1068. |

We thus find a decade time of roughly (1068-90)/10 ≈ 100 timesteps. The corresponding growth rate is comparable to the betatron frequency. Plots of this quantity for a similar run are shown in Fig. 5, discussed below.

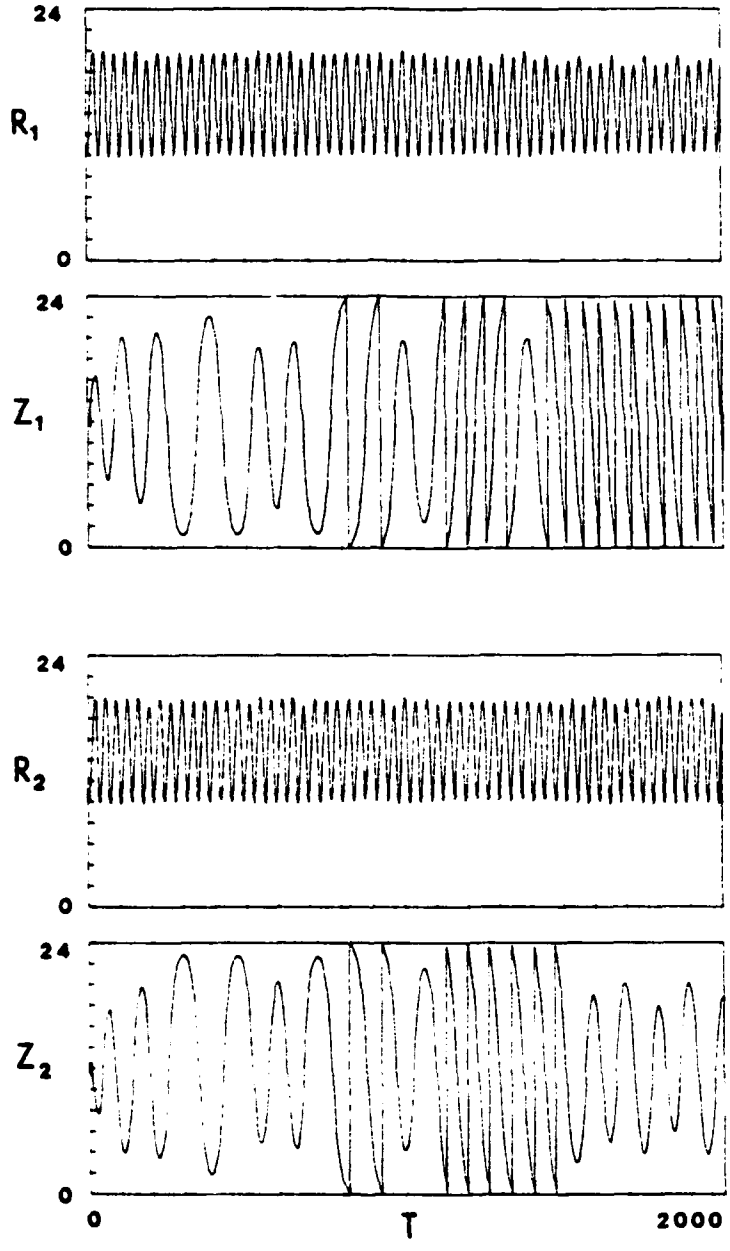


2. The orbits of a pair of particles which were initially a mirror image pair, selected from run JWA with EPS = $10^{-13}$. The histories of r and z as functions of time are shown. Mirror symmetry about Z = L/2 is evident until approximately timestep 1100.

To further verify that we are not simply observing a code "bug", runs were carried out using other values of the zero order fieldsolver convergence criterion, EPS. Run "JYA" used EPS = $10^{-11}$; for this run a difference was visible (on a large copy of Fig. 3) at about IT = 1075. This is not much earlier than in JWA, but recall that the growth is noisy and that absolute precision of the computer is about 14 digits, so that JWA's value of EPS probably cannot give much better accuracy than the less stringent value used in JYA. To see the effect more clearly, another run, "KAA", was made using EPS = $10^{-9}$ (see Fig. 4). For this run differences between the mirror image particles are visible at roughly IT = 825. This is about 250 timesteps earlier than in run JYA; since this run had an initial perturbation roughly 100 times as large as JYA, it would be expected to need two decades, or on the order of 200 timesteps, less growth for the separation to be visible. This appears to be consistant with the value of 250 observed.

Even though the orbits diverge greatly, energy conservation for both is excellent since only "rotations" of the velocity in the magnetic field are performed. However, since only $\underline{B}$ and not $A_\theta$ is used to advance the particle, it is hard to have a reliable measure of how well the canonical angular momentum is conserved. Using values of $A_\theta$ from which $\underline{B}$ was calculated by finite differences shows $P_\theta$ conservation to be valid within 5 or 10 percent, with $P_\theta$ oscillating without any change on a long timescale. However, this measure is somewhat unreliable, and the oscillations probably have no real meaning. In runs using a finer grid and smaller timestep the magnitude of these oscillations was less, but code behavior was similar.

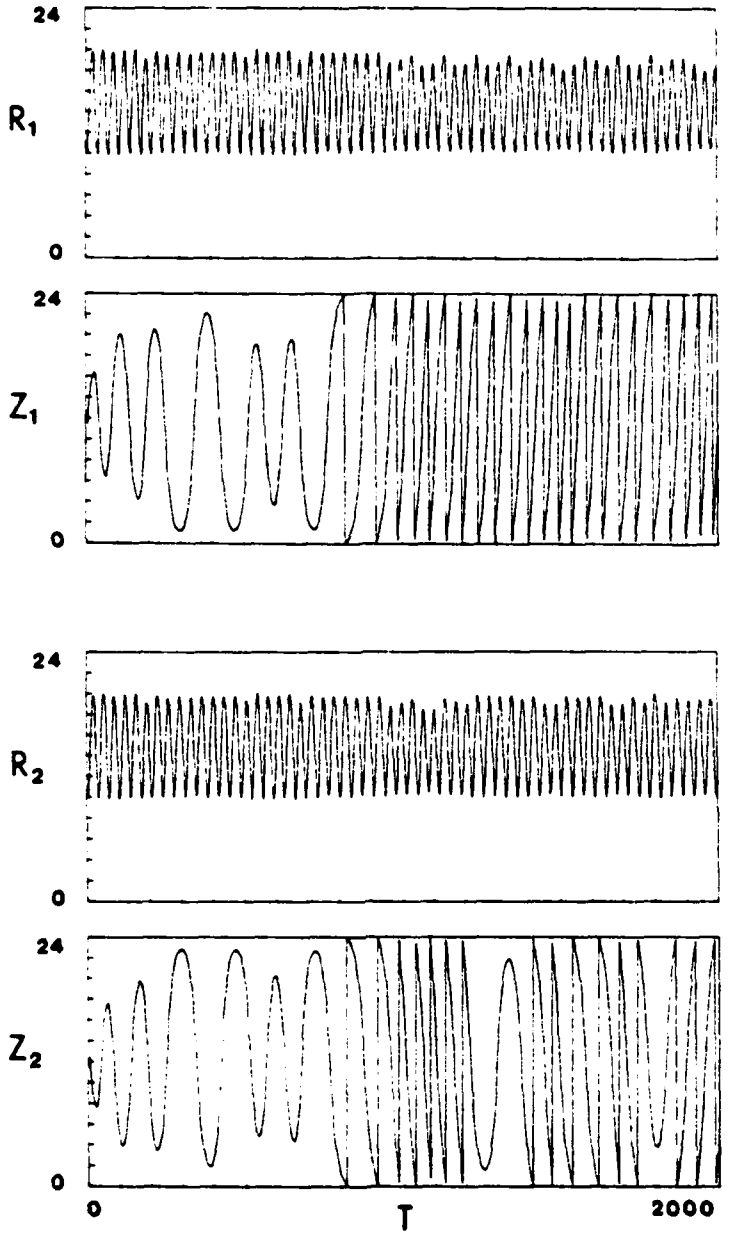


3. The same quantities from run JYA with EPS = $10^{-11}$. Symmetry holds until approximately timestep 1075.

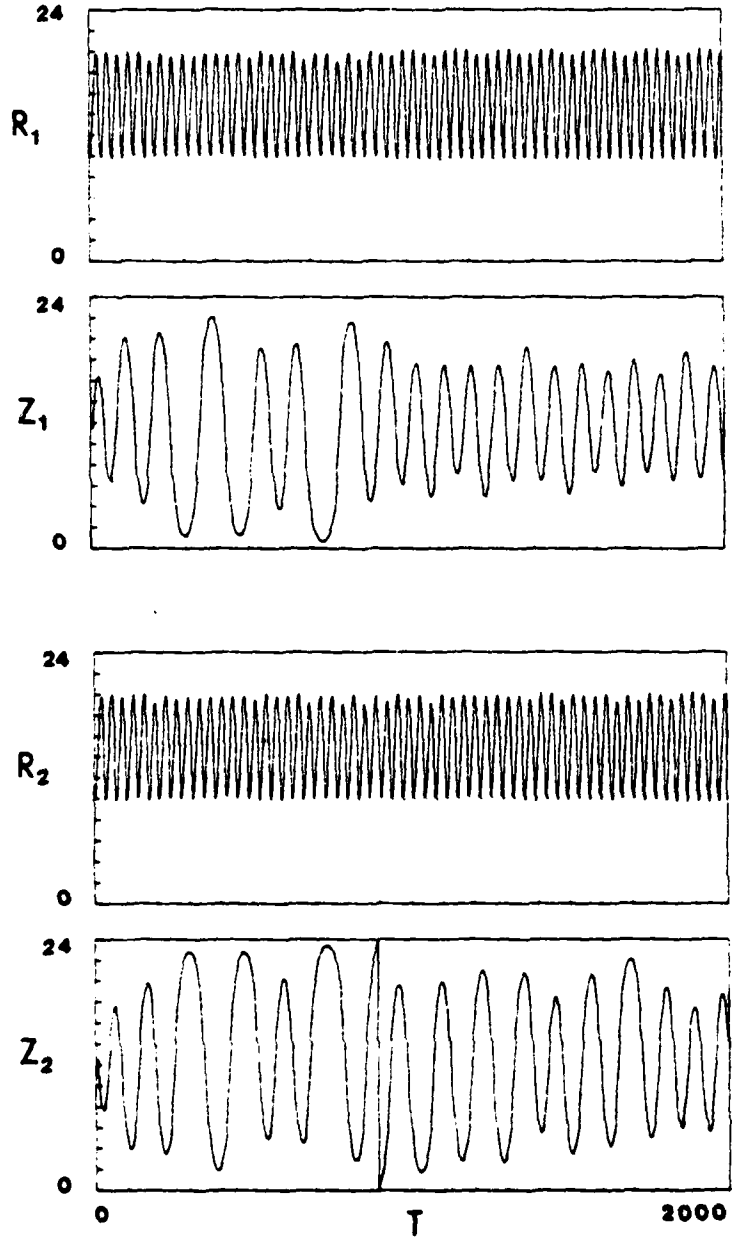


4. The same quantities from run KAA with EPS = $10^{-9}$. Symmetry holds until approximately timestep 825.

## B. Ergodicity and Confinement

The zero order effect eventually leads to a lack of symmetry of the ring; this is partly due to the small number of particles leading to fluctuations that only seemingly violate axial momentum conservation (consider a single particle in a mirror field - its axial momentum is not conserved). The effect is magnified by the periodic particle boundary condition; if one of the ex-mirror image pair of particles reaches the boundary at $z = 0$ or $L$, and the other does not, the center of mass of the ring shifts to one side or the other.

In addition, a particle may leave the ring (by entering the "loss cone") even after it has exhibited a large number of betatron oscillations within the confines of the ring; such a particle must be considered an "unconfined particle". An example is shown below wherein one particle was unconfined (first reached $z = 0$ or $L$) at timestep 2600, while its "mirror image" was confined until timestep 8400. The equilibrium fields of necessity include contributions from this class of particles. Lovelace has shown that exponential rigid rotor equilibria, for example, contain unconfined orbits [7], and therefore require sources and sinks of particles at $z = \pm \infty$.

There appears to be a correlation between whether or not a particle's orbit is unconfined and whether or not it is ergodic (as expected, since both are associated with high energy), but it is not one-to-one. That is, some apparently confined particles show ergodic

motion - one cannot be sure they are in fact confined without making an infinitely long run, at least with the usual scheme of injection wherein random velocities are added to the injected particles (in a mirror - symmetric manner). Most recently, a run (KKA) was made wherein no random velocities were added. In this run each group of injected particles could only self-pinch together, and lose energy due to the inductive electric field when succeeding groups of particles were injected. Thus, all particles were necessarily confined (this was observed to be the case); nonetheless, the ergodicity - induced assymmetry was present in this run. Note that this method of injection gave an equilibrium which was not at all like a rigid rotor in that the angular velocity showed high shear.

On theoretical grounds one expects a different relationship between confinement and stochasticity depending upon whether the particle orbit encircles the axis (ion ring case) or does not (small-orbit mirror plasma, most particles). In the former, the level surfaces of the effective potential are closed, so that particles of small enough energy must be absolutely confined, while in the latter, the surfaces extend to infinity and confinement normally depends upon the particle pitch angle [9]. Jumps in the adiabatic invariant $\mu$ associated with stochasticity effectively enlarge the loss cone so that all stochastic orbits which do not encircle the axis are unconfined and should be excluded from the equilibrium [2]. However, for the ion-ring case (and for large orbit field-reversed mirrors as well) our experience suggests that an appreciable number of confined stochastic particles are generally present, at least when equilibria are formed by injection.

## C. System Length and "Unfrozen" Fields

Runs were made using a larger number of cells axially (a larger vacuum region on each side of the ring, and a longer periodicity length - the cell size was kept constant). Run "JZA" used 48 cells in z, while "KBA" used 96 cells. In general, we observed that the longer the periodicity length, the longer it took for the (same) two test particles to show assymmetry. Note that assymmetry showed up in the latter run even though the test pair did not reach the axial boundary during the run, but took nearly to timestep 2000 to do so, in contrast with the shorter systems described above wherein assymmetry was visible after about 1000 steps. Presumably this change in the rate of growth of assymmetry occurs because the shape of the effective potential well is different for the various system lengths, both due to the boundary condition on the fieldsolver being imposed at different places and due to the fact that in the axially short runs the particle periodicity condition was enforced more often during the setting up of the equilibrium fields. We do not anticipate that making the system longer still would reduce the ergodic behavior to any great degree, since the 96-cell system is already much longer than the ring, but have not verified this conjecture.

For the axially long systems, the axial halfwidth of the ring was observed to increase at long times both more rapidly and to a larger value than in the shorter systems (with similar rings but different "tanks"). Presumably this is due to the fact that when particles find their way into the "loss cone" they have a larger distance to travel

before reentering the ring region one axial period later, and so the halfwidth can grow appreciably. The growth in axial length is associated with unconfined (high energy) particles, and so tends to be present when ergodic orbits are present.

The breaking of mirror symmetry, and the axial halfwidth growth as well, were present even in a run wherein the zero order fields were never "frozen"; in fact the halfwidth growth was somewhat more pronounced in this case. We conclude that keeping fields "unfrozen" does not reduce the effects of ergodic orbits.

## D. Implications

We believe this loss of symmetry has not been noted previously in simulations of field-reversed ion rings and mirror plasmas, although it may have been present in runs of RINGA [10,11] or SUPERLAYER [12]. Normally, small deviations from symmetry (in runs where symmetry would be expected) are not measured in such simulations, and in a nonlinear 2D3V code these are the only quantities which grow exponentially. Also, "saturation" of this effect must set in when the amplitude becomes comparable to the system size, or perhaps more properly to a smaller "island width" of the ergodic region in the r-z projection of phase space [2]. Figure 5 shows the quantities $|r_1-r_2|$ and $|z_1+z_2-L|$ plotted as functions of time for a run with L = 96. The last three decades of exponential growth, and the "saturated" state, can be seen. Here

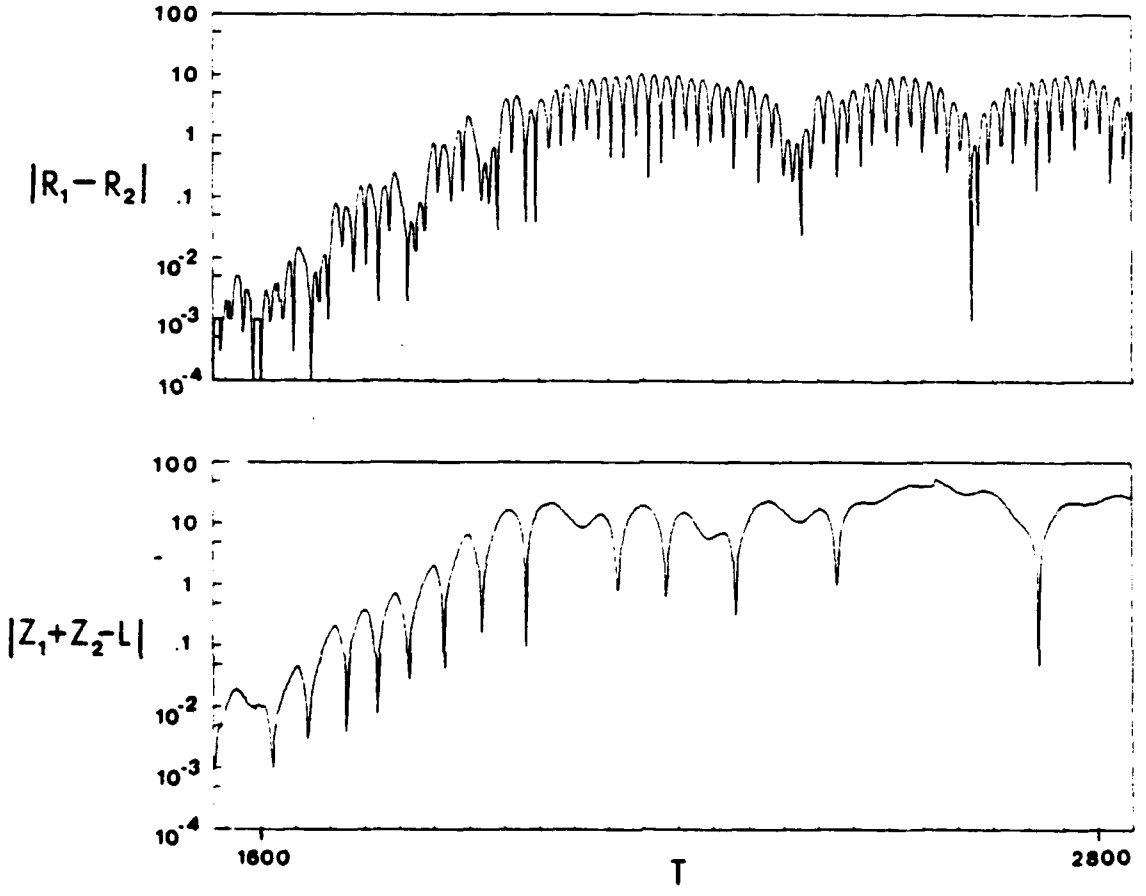


5. Plot of $|r_1-r_2|$ and $|z_1+z_2-L|$ as functions of time for a run with L = 96. The maxima of these quantities are seen to be of order the system size.

"saturation" appears to occur when the separation of the orbits is of order the system size.

The loss of symmetry to zero order probably is not of great fundamental consequence by itself. One could simulate only the region Z > L/2 for example, enforcing the mirror symmetry for all time, if one were only interested in the zero order ring behavior.

## III. SURFACES OF SECTION AND ERGODICITY

To confirm that we are in fact observing both nonergodic and ergodic orbits, surface of section plots were generated. These show the particular values taken by r and $\dot{r}$ of each particle as the particle passes through z = L/2. Such plots, and variations using other variables, have been employed previously to show orbital ergodicity [1]. They depict a "slice" of the phase space through which the particle trajectory moves. If the particle orbit is to sweep out a nonzero volume of this space, it must also sweep out a nonzero area of the slice. To make the plots, a postprocessor program was written. It extracted the tracer particle histories of r and z as functions of time from a printed output file, which was generated by RINGHYBRID and rearranged using a text editor. The program computed the instants of time at which z = L/2 was crossed using linear interpolation on the history of z. Again using linear interpolation, the values of r at these same instants were calculated from the r history. Finally, the

associated values of $\dot{r}$ were calculated by a simple finite difference. While this interpolation scheme is of low order, it appears to be reasonably effective when small timesteps are taken and the histories are arranged so as to save every point of the trajectory. Furthermore, it can be argued that the simple leapfrog mover used by the code does not justify a higher-order interpolation scheme, though this point is not entirely clear.

Illustrated in Fig. 6 are the r and z histories of a nonergodic particle selected from a run with L = 96. The plot shows the trajectory over 8000 timesteps, a very long run for the code. In Fig. 7 the surface of section plot for this particle is shown. Fields were "frozen" at timestep 450 and every other timestep was saved in the history file; the plot shows points taken from the interval between timesteps 452 and 8000. The plane z = L/2 was crossed 235 times during this time. Points in this plot are observed to fall on a crescent-shaped curve, without filling in the area of the crescent. There is, however, considerable raggedness to the plot, which may be ascribed to the finite timestep and the diagnostic interval of two. To demonstrate this, Fig. 8 shows a surface of section for the same particle using a diagnostic interval of one step and starting from timestep 451. The curve is seen to be much smoother than that of Fig. 7.

The orbit of an ergodic particle from the same run is shown in Fig. 9. The particle is not bound and the periodicity condition is enforced a number of times, the first time being approximately at timestep 2600. The surface of section plot for this particle is shown in Fig. 10. Diagnostics were made every timestep. For this trajectory

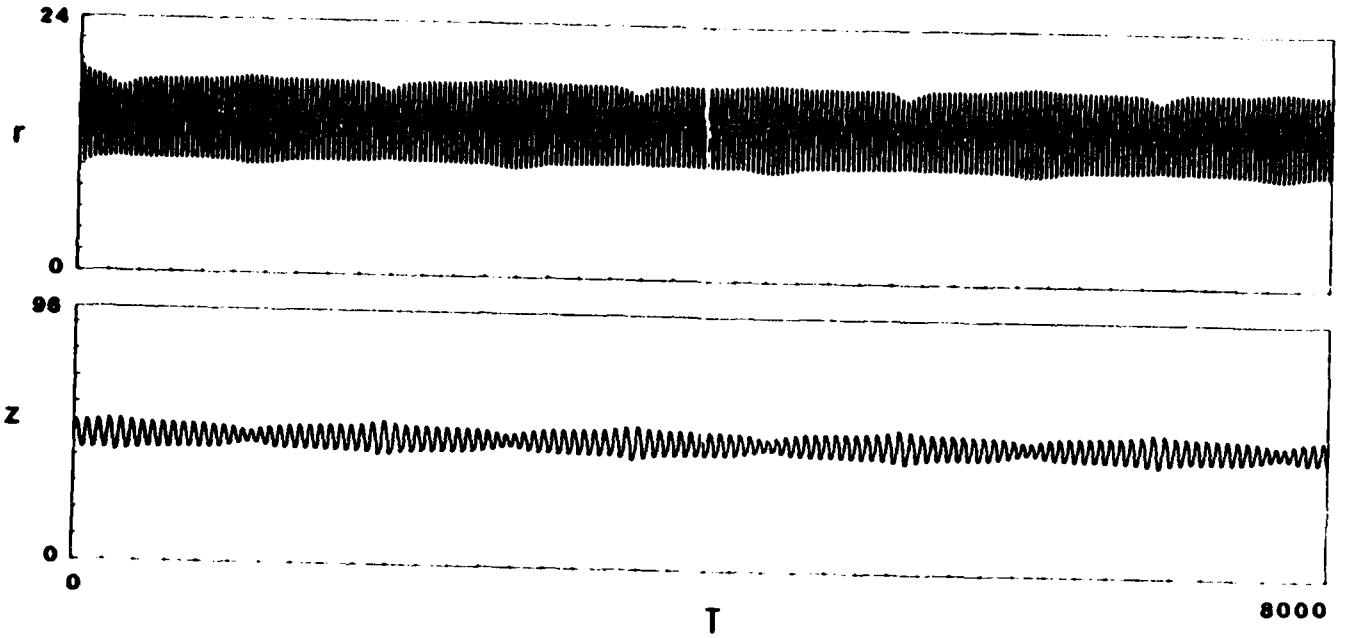


6. R and z histories for a nonergodic particle selected from a run with L = 96, over a period of 8000 timesteps.

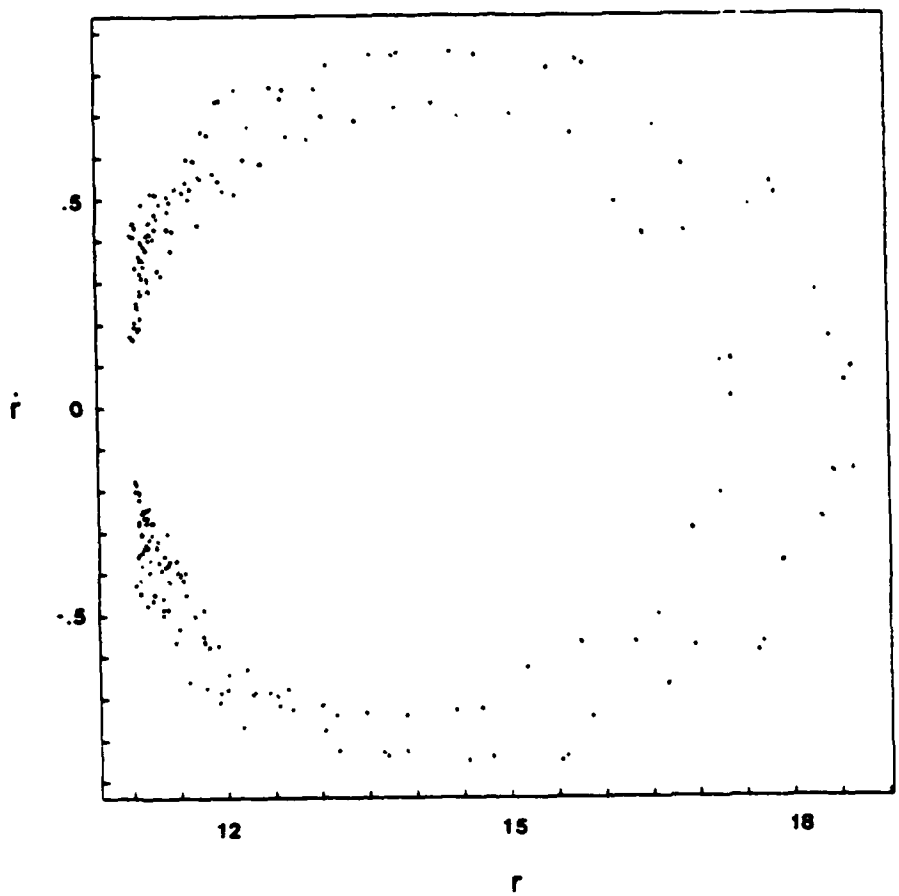


7. A surface of section plot for the particle of fig. 6, as described in the text. Diagnostics were performed every other timestep, and linear interpolation between these points was used. Note that points fall on a crescent but do not fill the area enclosed by the crescent.

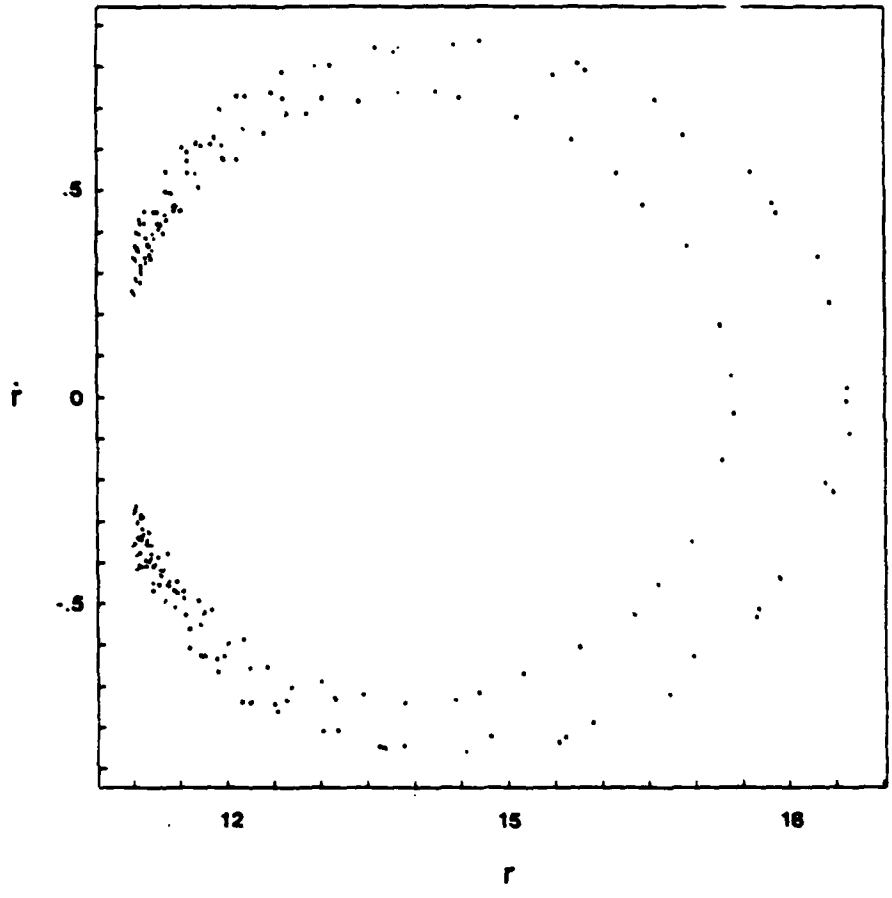


8. Another surface of section plot for the particle of fig. 6., but with diagnostics performed every timestep. Less spread in the pattern is evident.

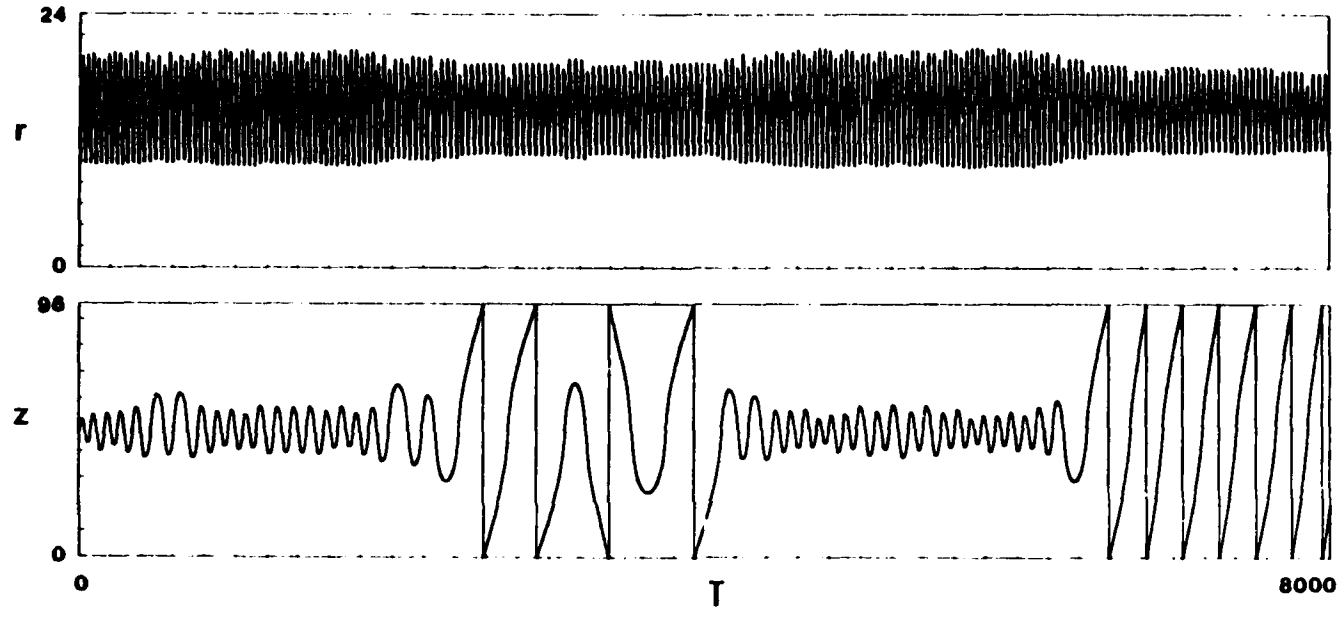


9. R and z histories for an ergodic particle from the same run.

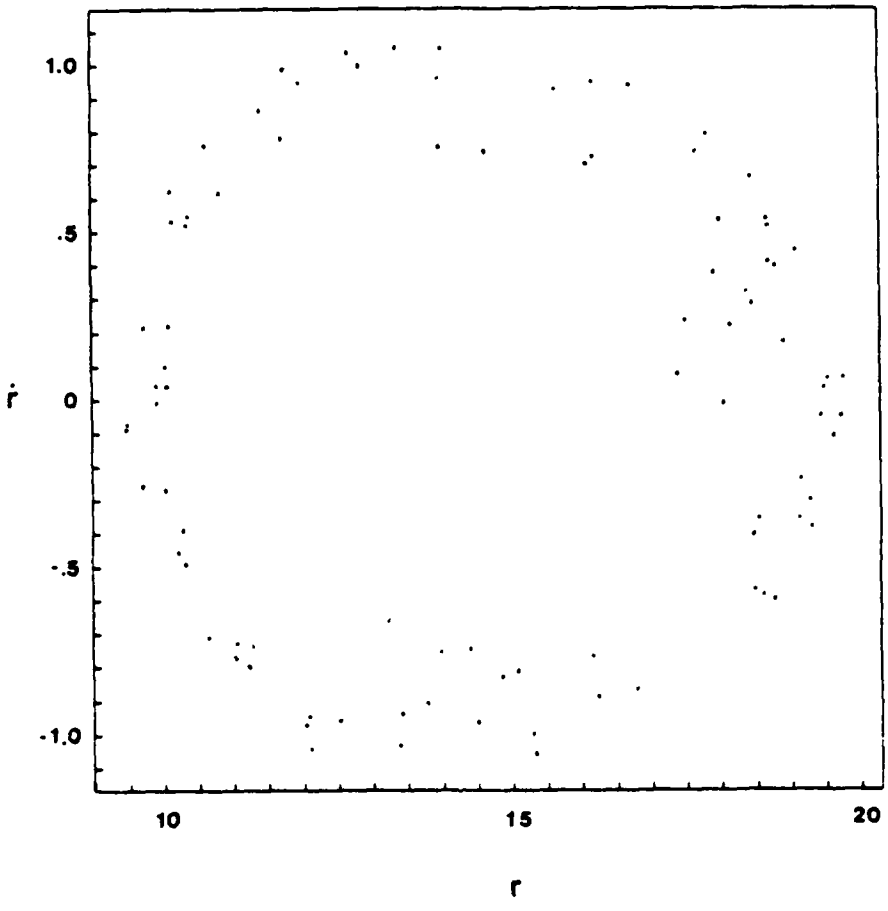


10. Surface of section plot for the ergodic particle of fig. 9. The points fill an annular region, and are not confined to the outline of a region as was the case for the particle of figs. 6 – 8.

there were 89 crossings of $z = L/2$. There is evidently a qualitative difference between this orbit and the previous one, as here the points do not lie on a smooth curve but appear to fill an annular region of the plane. The orbit of the particle that was initialized to be the mirror image of the particle in Fig. 9 is shown in Fig. 11. In contrast with its "mirror image", this particle appears to be bound for the 8000 timesteps illustrated. In fact, a continuation of the run shows this particle to be unbound, first reaching the end of the system at timestep 8400. It would be surprising were this not the case, as the same regions of phase space should normally be acessible to both of a mirror image pair of ergodic particles. The surface of section plot for this trajectory is shown in Fig. 12; in fact, this plot and that of Fig. 10 might be superposed to give a clearer picture of the area of the $r - \dot{r}$ plane accessible. There were 154 crossings of $z = L/2$ in this case.

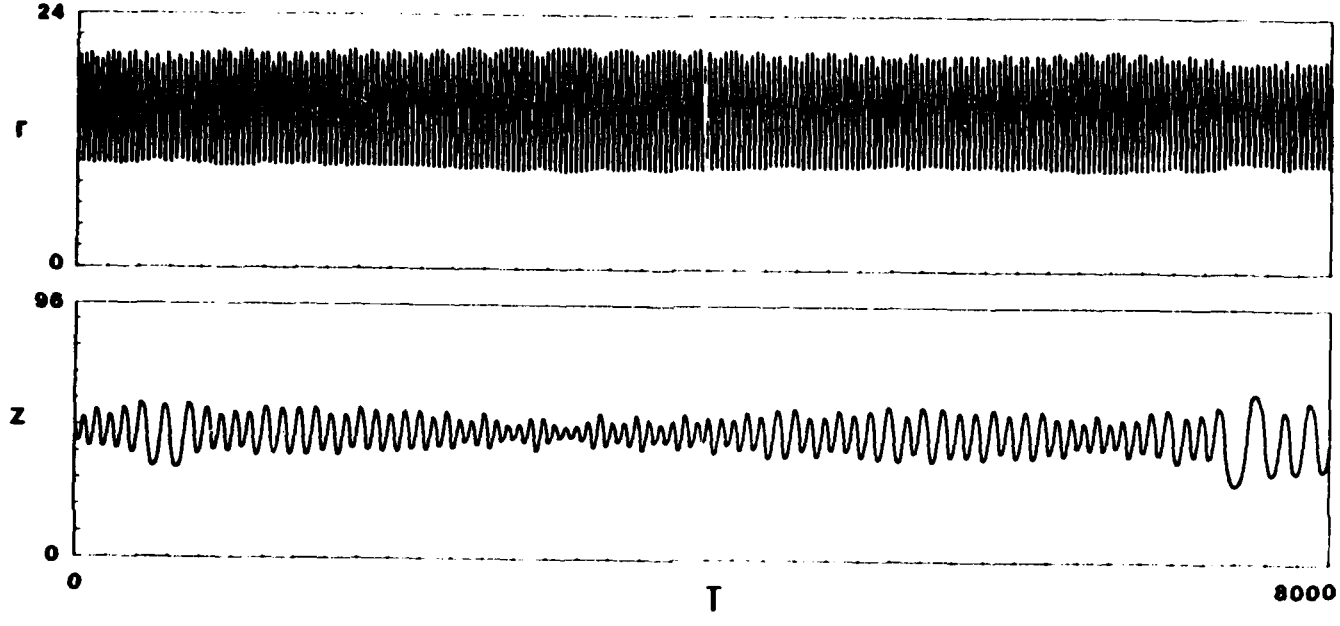


11. R and z histories for the particle that was initially the mirror image of the particle of figs. 9 and 10. This particle appears to be confined – in fact it becomes unconfined at timestep 8400, beyond the end of this plot.

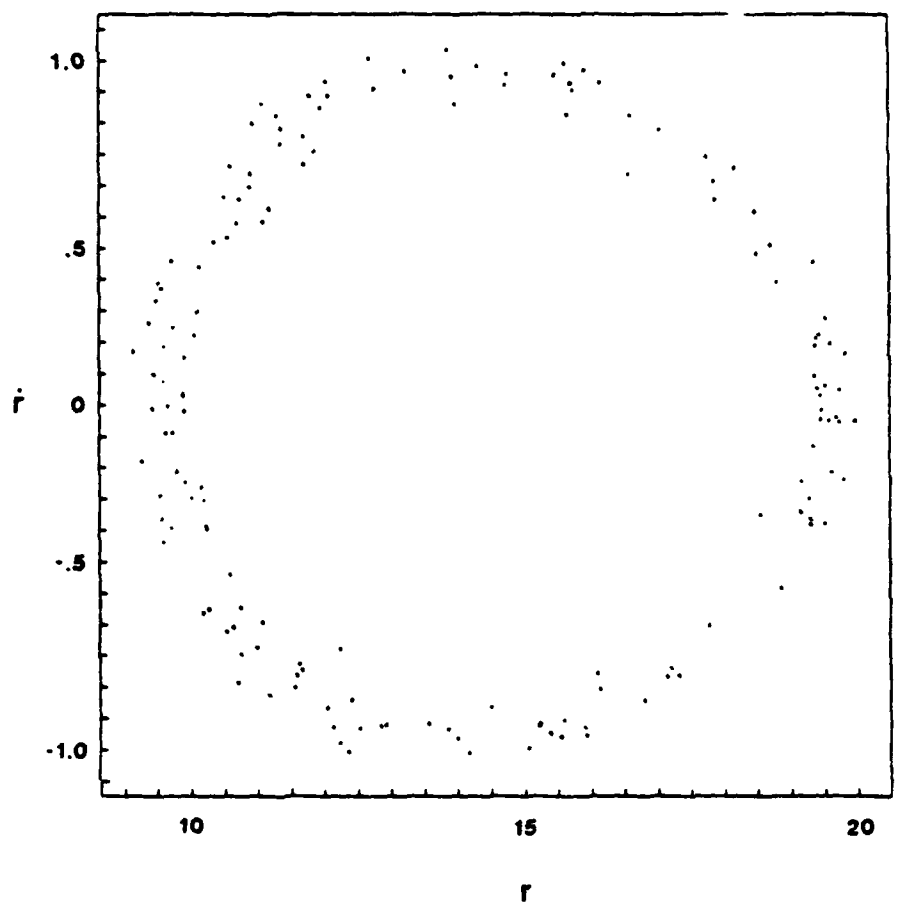


12. Surface of section plot for the particle of fig. 11.

# IV. EFFECTS UPON THE LINEARIZED SIMULATION

## A. Observation

The second manifestation of the diverging trajectories is of much greater fundamental concern. In the first order linearization, we consider the motion of a "displaced point" P′ relative to that of an unperturbed point P [4]. The vector separation between the two is denoted as $\underline{\varepsilon}$. Since the points P and P′ represent neighboring trajectories, when orbits are ergodic we can expect the magnitude of $\underline{\varepsilon}$ to increase exponentially with time whether or not Eulerian first-order fields are included in the calculation, since the stochastic growth is due to particle motion in the inhomogeneous zero order field. This is in fact the observed behavoir.

Figure 13 shows part of a non-ergodic particle orbit (r and z versus time) selected from a run with the parameters of KBA. This is the same particle plotted in Fig. 6; timesteps 2000 to 4000 are shown here in detail. For this particle, time histories of the magnitudes of the r, $\theta$, and z components of $\underline{\varepsilon}$ are plotted in Fig. 14. The initial excitation was implemented by giving all particles a positive first order axial velocity $\dot{\varepsilon}$ at timestep 500, and no Eulerian first-order fields were included in the calculation. All components of $\underline{\varepsilon}$ are seen to oscillate steadily. This may be contrasted with the behavior of the ergodic particle of Fig. 9, part of the orbit of which is shown in greater detail in Fig. 15. As seen in Fig. 16, all components of $\underline{\varepsilon}$ grow

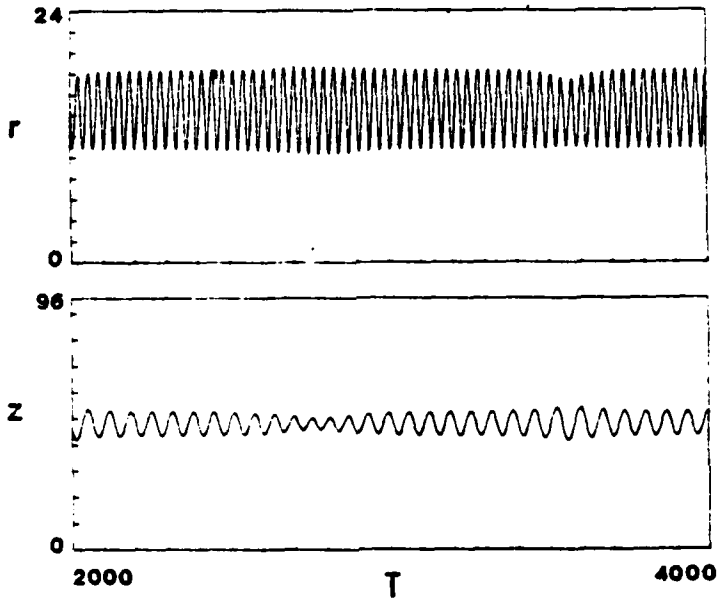


13. Expanded r and z histories for the nonergodic particle of figs. 6 - 8.

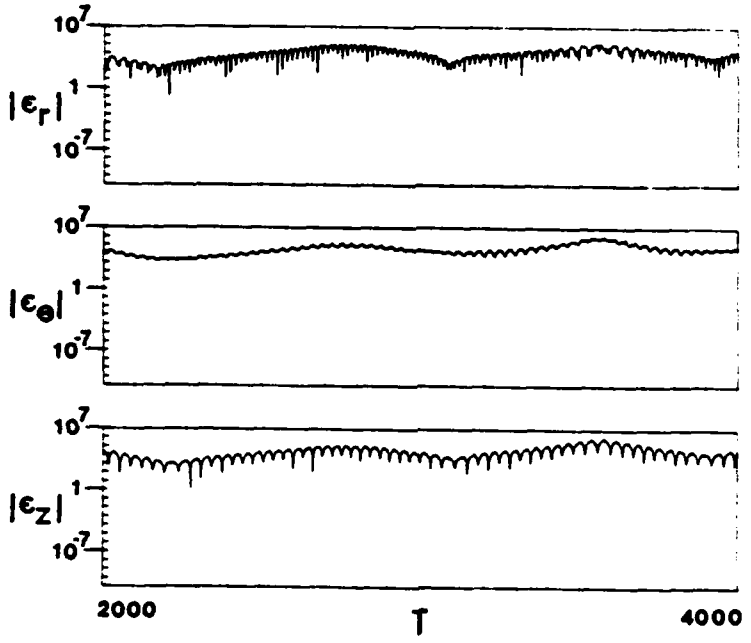


14. Time histories of the magnitudes of the r, $\theta$, and z components of $\underline{\varepsilon}$ for the nonergodic particle of figs. 6 – 8 and 13.

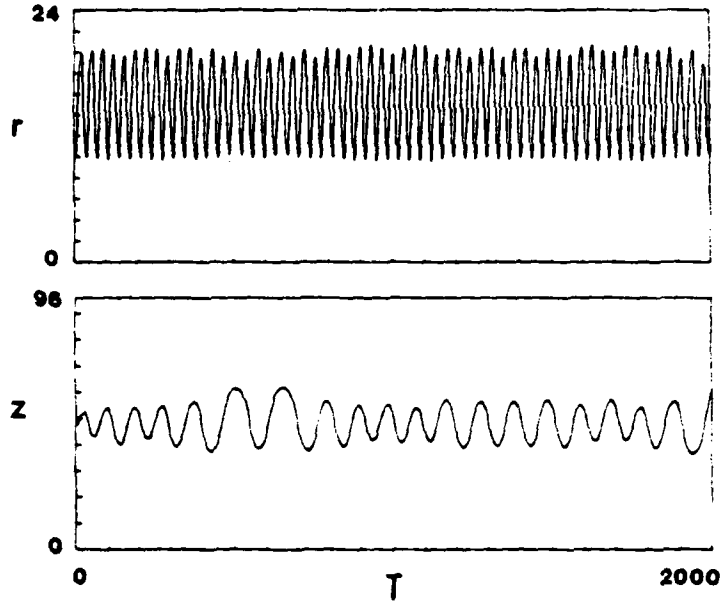


15. Expanded r and z histories for the ergodic particle of figs. 9 and 10.

noisily. Figure 17 shows the time histories of the components of the mean $\underline{\varepsilon}$ obtained by averaging over all particles. The mean $\varepsilon_z$ shows stable oscillation at first, as would be expected without any first order field response to drive kink modes etc., but soon the ragged growth characterizing the single-particle modes takes over. The r and $\theta$ mean components are initially zero due to the symmetry of the first order initialization. As symmetry breaks down they grow rapidly to a level comparable to that of the z component, then grow at the same (slower) rate as the latter. This is because the three components of $\underline{\varepsilon}$ are mutually coupled for each particle, as seen in the previous figure. The growth is even faster in runs with a shorter periodicity length L.

When the term $\underline{v}_0 X(\underline{\varepsilon}\cdot\nabla)\underline{B}_0$ in the linearized equation of motion is deleted, the first order motion is observed to become stable. To understand this lack of growth note that, using the linearized equation of motion,

$$d/dt[(\underline{v}_0+\dot{\underline{\varepsilon}})^2] = 2\dot{\underline{\varepsilon}}\cdot[\underline{v}_0 X(\underline{\varepsilon}\cdot\nabla)\underline{B}_0],$$

so that $\dot{\underline{\varepsilon}}$ cannot grow indefinitely when the right hand side is zero. This term is responsible for making the orbit of P′ a neighboring orbit to that of P, and not an identical orbit as when the term is omitted.

Because of the relationship between high energy (large excursion) and ergodicity, an attempt was made to eliminate the large-excursion particles by placing "sticky" walls at Z = 6 and 18, in a run with L = 24. While 400 of the 2400 particles were removed, stochastic growth of $\underline{\varepsilon}$ was still present, and the maximum growth rate was only slightly less than in the comparable run made without the sticky walls. See also

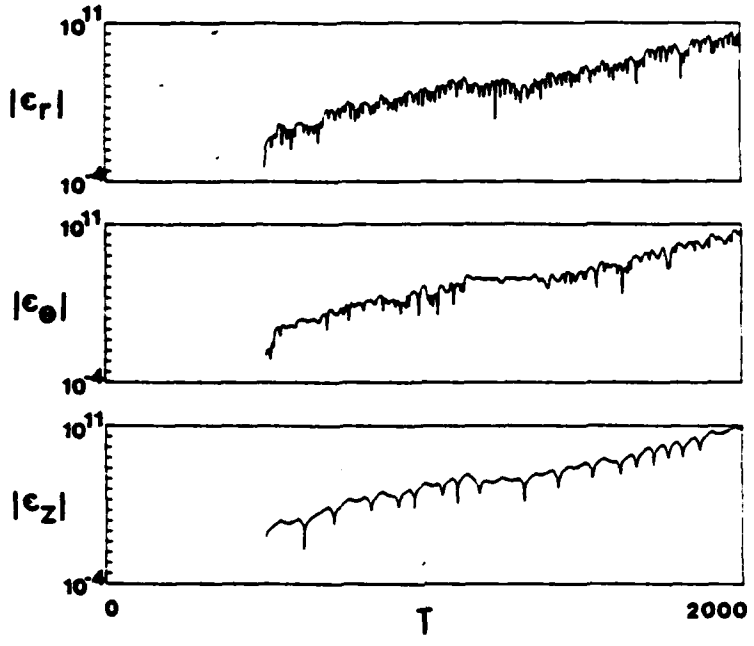


16. Time histories of the magnitudes of the r, $\theta$, and z components of $\underline{\varepsilon}$ for the ergodic particle of figs. 9, 10, and 15. Noisy growth is evident.

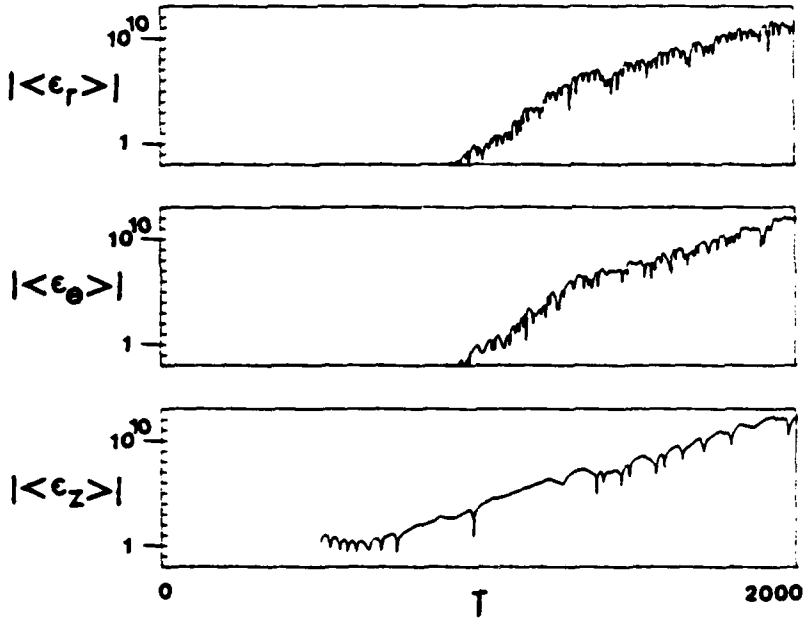


17. Time histories of the magnitudes of the mean r, $\theta$, and z components of $\underline{\varepsilon}$ obtained by averaging over all particles.

the discussion of run KKA in the section above on ergodicity and confinement.

## B. Implications

This type of dynamical instability is quite distinct from the collective plasma effects we wish to examine. In a true Vlasov plasma with an infinite number of particles, the random phases of the growing displacements $\underline{\varepsilon}$ for all particles would be expected to cancel out in the mean, and no gross plasma moments would be affected. However, in a simulation plasma with perhaps one to ten thousand particles, this may not be the case. Since different particles have different growth rates, the single-particle growth of one or a few particles comes to dominate, and when we examine moments such as mean $\underline{\varepsilon}$, first order currents, etc. the only thing that appears is the effect of this one or few particles. Unless the collective modes have a higher growth rate than the fastest growing single particle mode, only the latter can be seen, and regardless of background plasma parameters the growth will appear the same.

If one attemts to minimize the stochastic growth by increasing the number of particles, the reduction is small since the cancellation should improve only as the square root of the number of particles. Attempts to reduce the mean rate of growth by employing up to 9600 particles were unsuccessful, possibly because when more particles were used some fell on orbits with even higher associated growth rates.

Presumably cancellation would occur if a far greater number of particles were employed.

J.M. Finn has observed, in computer experiments using model potentials, a strong model dependence of the ergodic properties. In two of three models, including one self-consistant model, he observes predominantly ergodic behavior, while in the last (nonself-consistant) model he observes only limited ergodic behavior. D. A. Larrabee and R. V. Lovelace, using a different self-consistant model not described in detail, find ergodic orbits to be present only in one "highly compressed" ring [3]. By suitable choice of model it may thus be possible to find equilibria with only weak single-particle growth, or none at all. This may present a serious restriction on the class of problems which can be run. Discrete representations of numerically calculated Vlasov equilibria may prove useful, since equilibria formed by injection, as in RINGHYBRID, are rather likely to encompass ergodic orbits. However, even some equilibria formed by injection can be expected to prove usable; recent results suggest that in one fully field reversed ring with an aspect ratio of order 4:1 the ergodic growth is slow enough that meaningful conclusions about collective behavior can be drawn from the results.

It may be possible to treat problems involving ergodic orbits by other means. Perhaps the fastest-growing particles can be removed from the computation artificially, at some risk of affecting the physics. This may be most reasonable for mirror plasmas where only a small fraction of the particles are both axis-encircling and ergodic. It may be possible to reconstruct the distribution function $f^1$, and possibly $f^0$, periodically in a moment-conserving manner, as a possible means of

smoothing out the single-particle effects [13]. Finally, it may be possible to obtain results on collective behavior by somehow "subtracting" a run made without any first-order field response, such as the run illustrated, from one with full plasma response. The problem with the latter approach is that any errors in the subtraction also grow exponentially, and it is probably impossible to get amplitude and phase of the single particle modes in the two runs aligned with each other.

## V. CONCLUSIONS

In summary, the effects of ergodic single-particle orbits have been observed in a series of computer simulations of strong ion rings. It is anticipated that they are also present in a wide class of systems such as field-reveresed mirror plasmas with large nominal gyroradius. Nonlinear 2D3V codes are able to treat problems involving ergodic orbits with only minor difficulties. These include an eventual violation of mirror symmetry and small fluctuations in a normally conserved momentum. Linearized codes, however, are more severely affected by the presence of ergodic orbits. The exponential growth of the displacement between unperturbed and perturbed trajectories can be sufficiently rapid as to mask the collective modes which are the true objects of study. Fully nonlinear 3-D codes may also experience difficulties when ergodic orbits are present; the mode being studied may saturate at a lower level than that associated with the stochastic growth. At present we know of no

way to eliminate the undesirable single-particle modes when ergodic orbits are present; however, it is possible that by careful choice and implementation of equilibria, linearized simulations will still prove applicable to a wide class of problems.

## ACKNOWLEDGMENTS

The author wishes to acknowledge useful discussion with C. K. Birdsall, J. A. Byers, R. H. Cohen, J. Denavit, J. M. Finn, M. J. Gerver, and R. N. Sudan. The encouragement afforded by Prof. Birdsall is appreciated.

This work was supported by the U. S. Department of Energy Contract DE-AS03-76SF00034, Project Agreement DE-AT03-76ET53064.

## REFERENCES


1. J. M. Finn, "Stochastic Behavior of Particle Orbits in Field Reversed Geometries," Plasma Phys. 21, 405 (1979).
2. R. H. Cohen, private communication.
3. D. A. Larrabee and R. V. Lovelace, paper no. 1C39, Proc. of the Sherwood Meeting on Theoretical Aspects of Controlled Thermonuclear Fusion, Mt. Pocono PA, April 18–20 (1979).
4. A. Friedman, R. N. Sudan, and J. Denavit, paper no. PC–13, Proc. of the Eighth Conf. on Numerical Simulation of Plasmas, Monterey CA, June 28–30 (1978);
   "A Linearized 3–D Hybrid Code for Stability Studies of Field–Reversed Ion Rings," Cornell University Lab. of Plasma Studies Rept. no. 268 (1979), submitted to J. Comp. Phys. (1979).
5. A. Friedman and R. N. Sudan, Cornell University Lab. of Plasma Studies Rept. no. 237 (1978).
6. R. V. Lovelace, Phys. Fluids 19, 723 (1976).
7. R. V. Lovelace, D. A. Larrabee, and H. H. Fleischmann, Phys. Fluids 21, 863 (1978).
8. R. V. Lovelace, D. A. Larrabee, and H. H. Fleischmann, Phys. Fluids 22, 701 (1979).
9. G. Schmidt, Physics of High Temperature Plasmas, Pp. 29–44, Academic Press, New York (1966).

10. A. Friedman, R. L. Ferch, R. N. Sudan, and A. T. Drobot, Plasma Phys. 19, 1101 (1977).

11. A. Mankofsky, A. Friedman, and R. N. Sudan, Cornell University Lab. of Plasma Studies Rept. no. 245 (1978).

12. M. Brettschneider, J. Killeen, and A. A. Mirin, J. Comp. Phys. 11, 360 (1973).

13. J. Denavit, private communication.